Transmission of 96 × 100-Gb/s Bandwidth-Constrained PDM-RZ-QPSK Channels With 300% Spectral Efficiency Over 10610 km and 400% Spectral Efficiency Over 4370 km

Jin-Xing Cai, *Fellow, IEEE, Member, OSA*, Yi Cai, *Member, IEEE*, Carl R. Davidson, Dmitri G. Foursa, *Senior Member, IEEE*, Alan J. Lucero, Oleg V. Sinkin, *Member, IEEE*, William W. Patterson, Alexei N. Pilipetskii, Georg Mohs, *Senior Member, IEEE*, and Neal S. Bergano, *Fellow, IEEE, Fellow, OSA*

***Abstract*—We demonstrated that simple pre-filtering at the transmitter to constrain the channel bandwidth together with a maximum *a posteriori* probability (MAP) detection algorithm can significantly improve spectral efficiency (SE). 96 × 100-Gb/s bandwidth-constrained polarization-division-multiplexing return-to-zero-QPSK channels were transmitted with 300% SE over 10 610 km using 52-km spans of 150-μm ^{2} fiber and simple single-stage erbium-doped fiber amplifiers without any Raman amplification. We also achieved 400% SE over 4370 km using similar techniques.**

***Index Terms*—Coherent communications, inter-channel interference, intersymbol interference (ISI), maximum *a posteriori* (MAP) estimation, optical fiber communications, phase-shift keying (PSK), polarization-division multiplexing (PDM), wavelength-division multiplexing (WDM).**

I. Introduction

THE virtually insatiable demand for capacity has driven the research community to focus on transmission experiments with higher data rates and increased spectral efficiency (SE). However, high data rates ($\geq$100 Gb/s) and high SE ($\geq$200%, i.e., >2 bits/s/Hz) are particularly challenging for transoceanic cable systems. With the advent of digital coherent receivers, several impressive transoceanic 100-Gb/s experiments with high SE have been demonstrated. In the past year, we have seen transoceanic transmission demonstrations with 200% SE using the 100-Gb/s single-carrier polarization-division multiplexing (PDM)-QPSK modulation format [1], [2] or the 100-Gb/s two-carrier PDM-QPSK modulation format [3]. Furthermore, SE enhancement ($\sim$360%, i.e., 3.6 bits/s/Hz) was demonstrated with more elaborate PDM-OFDM techniques [4]. For all the aforementioned demonstrations, either Raman assisted erbium-doped fiber amplifiers (EDFAs) or pure Raman amplification was used to boost the received optical SNR (OSNR) for the 100-G signals.

In our study, we transmitted 96 × 112-G PDM-RZ-QPSK channels that were bandwidth constrained by pre-filtering over a 10610 km path constructed with an amplifier chain consisting of single-stage EDFAs and 150-μm ^{2} large effective area fiber with 52-km amplifier spacing [5]. We achieved 300% (i.e., 3 bits/s/Hz) SE with >10 dB Q-factor for all 96 channels. In addition, we also achieved 400% (i.e., 4 bits/s/Hz) SE over 4370 km again using bandwidth-constrained PDM-RZ-QPSK. Both results were accomplished without differential decoding. The aggressive pre-filtering required for both demonstrations created significant back-to-back intersymbol-interference (ISI) penalty that produced a complex signal constellation and can be interpreted as symbol correlation in the modulation format [14]. We have developed a suite of coherent detection algorithms including a maximum *a posteriori* probability (MAP) detection algorithm [9], [14] to take advantage of the symbol correlation to mitigate the linear ISI penalty associated with the tight filtering. With > 3-dB MAP gain, we showed that > 400% SE is achievable using bandwidth-constrained PDM-RZ-QPSK transmission.

II. Experimental Setup

Fig. 1 shows a schematic of our 100-Gb/s PDM-RZ-QPSK transmitter setup. Four binary 28-Gb/s signals ($I, \bar{I}$, and $Q, \bar{Q}$ with pseudorandom binary sequence length $2^{23} - 1$) are electrically generated by multiplexing 14-Gb/s data streams from a four-channel pulse pattern generator. The 28-Gb/s streams are applied in pairs to the I and Q ports of two QPSK modulators to generate two optical QPSK signals at 28 Gbaud or equivalently 56 Gb/s. After RZ pulse carving, each of the two optical signals is then split into two equal data streams. One 56-Gb/s data stream is delayed with respect to the other to decorrelate the data patterns. The two decorrelated data streams are then orthogonally recombined using a polarization beam combiner, resulting in two 112 Gb/s PDM-RZ-QPSK signals.

Each of the two QPSK modulators imparts its data onto a comb of wavelengths to generate two rails of odd and even channels. The two rails are bandwidth constrained and combined with cascaded 33-GHz or cascaded 25-GHz optical interleaving

Manuscript received August 11, 2010; revised October 26, 2010; accepted November 08, 2010. Date of publication November 22, 2010; date of current version February 02, 2011.

The authors are with Tyco Electronics Subsea Communications LLC, Eatontown, NJ 07724 USA (e-mail: jcai@subcom.com).

Color versions of one or more of the figures in this paper are available online at http://ieeexplore.ieee.org

Digital Object Identifier 10.1109/JLT.2010.2093931

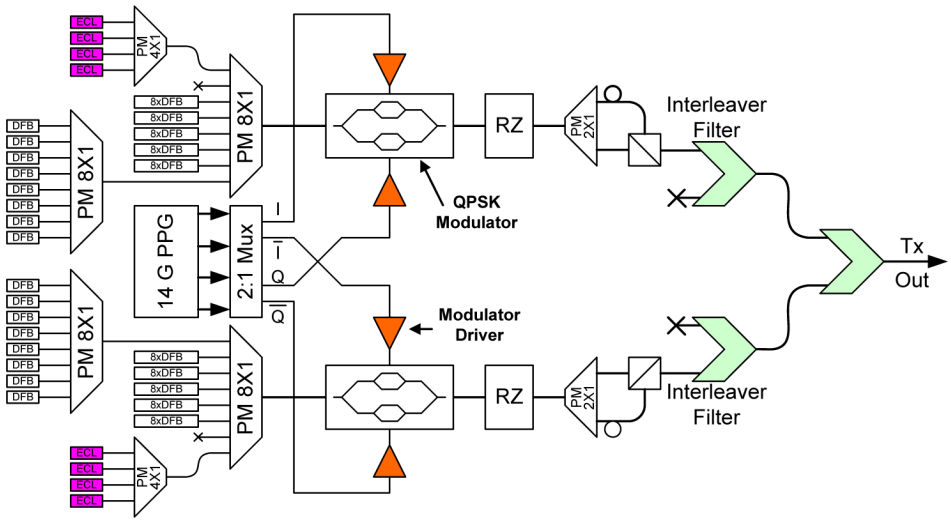

Fig. 1. 112-Gb/s bandwidth-constrained PDM-RZ-QPSK transmitter. DFB: distributed feedback laser, ECL: external cavity laser, Mux: electrical multiplexer, PPG: pulse pattern generator, PM: polarization maintaining, RZ: return-to-zero.

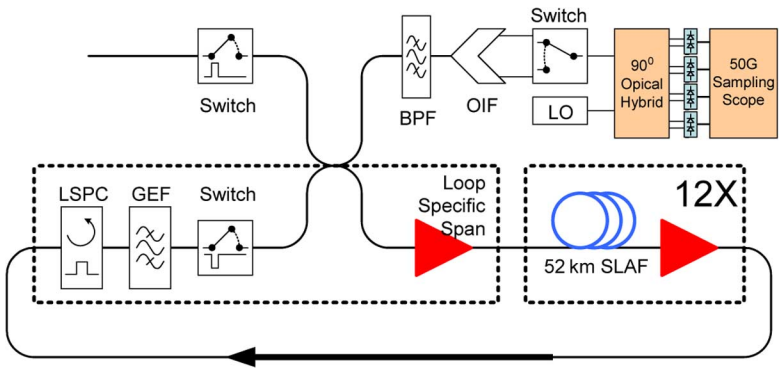

Fig. 2. Circulating loop testbed and 112-Gb/s PDM-RZ-QPSK receiver. BPF: tunable optical bandpass filter, GEF: gain equalization filter, LO: local oscillator, LSPC: loop synchoronized polarization controller, OIF: optical interleaving filter, SLAF: super large effective area fiber.

filters for 300% SE and 400% SE, respectively. Each rail consists of 48 DFB lasers and four tunable external cavity lasers (ECLs) with 1 pm resolution. The eight ECLs are tuned to a contiguous set of channels and the corresponding DFB lasers are disabled for the bit error measurements. This process is repeated and the ECLs are tuned across the band until all 96 channels are measured. All 96 channels are modulated in a similar fashion at all times.

The 624-km circulating loop testbed (see Fig. 2) consists of twelve 52-km spans using a super large effective area fiber (SLAF) with $A_{\text{eff}} \approx 150\ \mu\text{m}^2$, midband chromatic dispersion ≈20.6 ps/nm/km, and attenuation ≈0.183 dB/km. Each span is combined with a single-stage EDFA with 16 dBm output power and a gain equalized bandwidth of 26 nm. A loop specific section contains a loop synchronous polarization controller (LSPC) [6] and a gain equalization filter to compensate residual loop gain error. The average PMD of the loop is 1.7 ps. No pre-/post- or inline optical dispersion compensation was used in this experiment.

Our coherent-detection receiver (see Fig. 2) consists of cascaded interleaver filters (33 and 67 GHz or 25 and 50 GHz) followed by a tunable bandpass filter to demultiplex the channels and a polarization diversity 90° optical hybrid followed by four balanced detectors [7]. The electrical signals from the detectors are recorded using a digital sampling scope with 16-GHz analog bandwidth and 50-GS/s sampling rate. The recorded electrical signals are digitally processed offline.

III. Coherent Receiver Algorithms and ISI Reduction

All signal processing was performed offline. After waveform recovery and alignment, dispersion compensation was performed digitally in the Fourier domain. The resulting waveform was then resampled with the recovered clock. A constant modulus algorithm (CMA) was used for polarization tracking and PMD compensation. Carrier phase estimation was subsequently applied using the Viterbi-Viterbi algorithm [8]. The aggressive pre-filtering used to suppress WDM crosstalk (interchannel interference) resulted in significant intrachannel ISI penalty. This pre-filtering penalty was compensated using an MAP detection algorithm [14].

Fig. 3(a) shows transmission performance versus transmitter pre-emphasis for three different detection schemes (Ch50 after 10 610 km with 300% SE). In order to capture the full impact of linear and nonlinear interactions between neighboring channels, the power of eight contiguous channels was simultaneously changed (Ch50 being the sixth in the group of 8). PDM

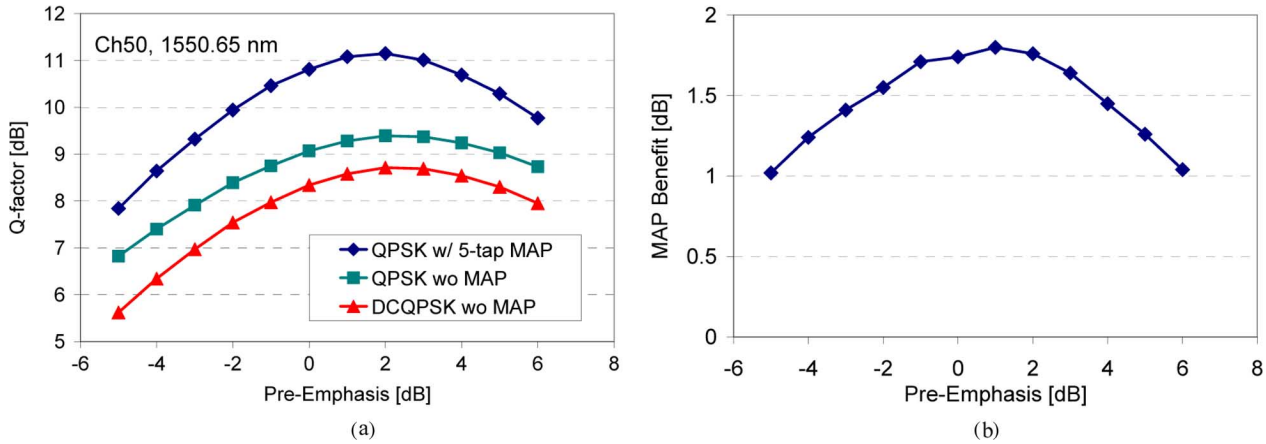

Fig. 3. (a) Q-factor versus transmitter pre-emphasis after 10610 km (300% SE) with pre-filtered PDM RZ-QPSK modulation format using three different detection schemes. (b) MAP benefit versus transmitter pre-emphasis after 10 610 km (300% SE).

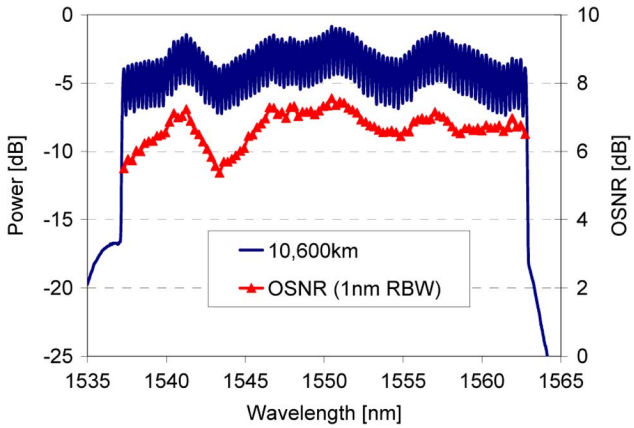

Fig. 4. Optical spectrum and OSNR (in 1 nm RBW) after 10 610 km.

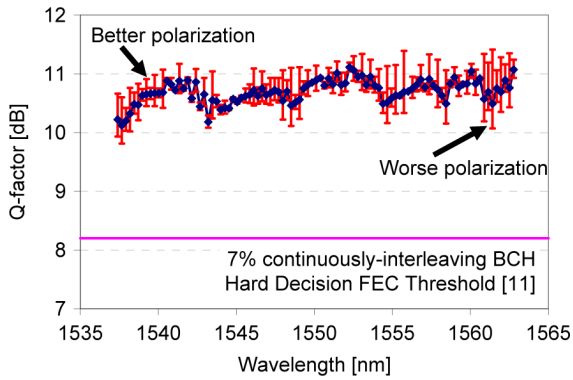

Fig. 5. Q-factor after 10 610 km (300% SE).

RZ-QPSK shows ∼0.7 dB better performance than differential coding PDM RZ-QPSK (DCQPSK); similar to results shown in [10]. Fig. 3(b) shows that the MAP benefit gradually increases as channel launch power is increased. At the optimum channel power, MAP detection provides ∼2 dB performance improvement after 10 610 km with 300% SE. As the channel becomes more nonlinear, the MAP benefit starts to degrade due to an insufficient number of taps to compensate the self-phase modulation (SPM)-induced ISI. 5-tap MAP was used for all measurements in this paper.

IV. 100-GHz Transmission Over 10 610 km With 300% SE Using Bandwidth-Constrained PDM-RZ-QPSK

The 96×112-Gb/s WDM signals were launched into the testbed without any individual channel power pre-emphasis. Fig. 4 shows the received spectrum and OSNR after 10 610 km (17 loops) with flat channel launch at the transmitter. The received OSNR in 1-nm resolution bandwidth (RBW) ranged from 5.4 to 7.6 dB with an average OSNR of 6.7 dB.

The BER of each channel was decoded from five sets of data with 2M samples each (2.35×10^7 bits/ch). Fig. 5 shows the Q-factor calculated from the average BER of the five datasets for each channel, together with the Q-factor of the two orthogonal polarizations. The average Q-factor for all 96 channels (total 2.25×10^9 bits of data decoded) was 10.7 dB, and the Q-factor of the worst channel was > 10.1 dB. The Q-factor difference between the two polarizations of a particular channel was attributed to polarization-dependent loss (PDL), and we observed up to 1.3 dB Q-factor difference between the two orthogonal polarizations. Even though the OSNR of Ch50 (see Fig. 4) was close to the highest among all 96 channels, the operating power for this channel was still ∼1 dB lower than the optimum channel power as shown in the power sweep measurements [see Fig. 3(a)]. Therefore, the performance of all channels could be further improved with increased EDFA output power. Fig. 5 also shows the forward error correction (FEC) threshold (8.2 dB) for a 7% continuously-interleaved BCH code [11]. Compared to this FEC, all channels had more than ∼2 dB average FEC margin.

In these experiments, we did not observe any cycle slips after decoding more than 2.25×10^9 bits at the 10 610-km transmission distance. We estimate that the probability of cycle slips in our experiments was less than 10^{-8} with more than 99% confidence, which is sufficiently low to be mitigated using some DSP algorithm such as the one described in [12]. An LSPC was used to ensure that the five datasets for each channel were measured with different polarization evolutions along the transmission line. Hence, time-varying PDL and PMD were included in all measurements.

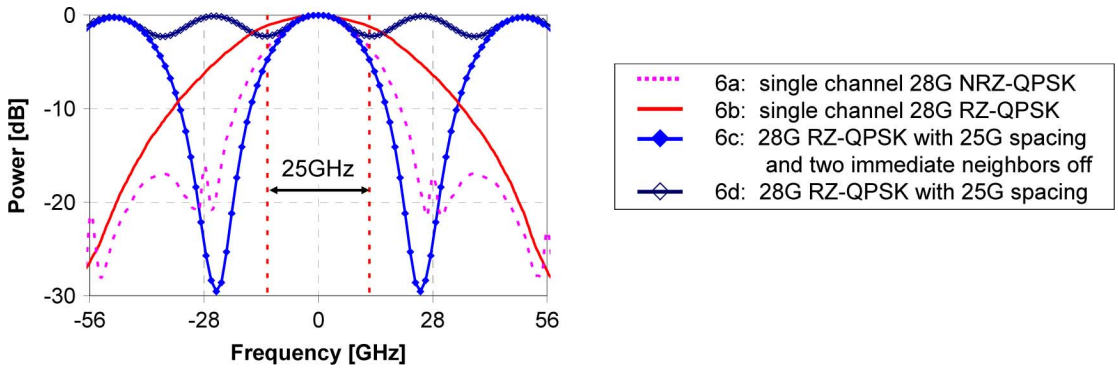

Fig. 6. Optical spectrum (single polarization) for 28-Gbaud RZ-QPSK, NRZ-QPSK, and bandwidth-constrained RZ-QPSK.

V. Bandwidth-Constrained PDM RZ-QPSK to Achieve 400% SE

To further explore the benefit of our MAP detection algorithms, we increased the SE to 400% by reducing the channel spacing to 25 GHz for the 28-Gbaud signals. All 33-GHz/67-GHz optical interleaving filters were replaced with 25-GHz/50-GHz optical interleaving filters. We use commercially available flat top optical interleaving filters with a combined pre-filtering BW of 15.6, 19.8, and 31.9 GHz at 1, 3, and 20-dB, respectively. Fig. 6 compares the optical spectra for a single-channel non-RZ (NRZ)-QPSK signal (6a), a single-channel RZ-QPSK signal (6b), RZ-QPSK signal that were bandwidth constrained using a 25-GHz optical interleaving filter at 50-GHz channel spacing (6c), and bandwidth-constrained RZ-QPSK signals at 25-GHz spacing (6d). Please note that all spectra in Fig. 6 are for single polarization only. The aggressive pre-filtering effectively removed crosstalk from neighboring channels (interchannel interference), as shown in Fig. 6. The spectrum of bandwidth-constrained RZ-QPSK (6c) is even narrower than that of NRZ-QPSK (6a).

While effectively limiting the crosstalk from neighboring channels, the aggressive pre-filtering also dramatically increased intrachannel ISI, and hence degraded the performance significantly. As shown in Fig. 7, the Q-factor at 10-dB OSNR was degraded from 15 dB (extrapolated) to 5.7 dB with the application of pre- and post-optical filters to a single-channel PDM-RZ-QPSK signal. Fig. 7 also shows the theoretical PDM QPSK performance limit. Compared with the theoretical limit, there is $\sim$1 dB OSNR penalty at 10-dB Q-factor using our experimental setup.

On the other hand, the pre-filtering-induced ISI can also be interpreted as intersymbol correlation and used in more advanced detection algorithms. It was shown in [13] that a joint-statistics sequence detection scheme can effectively reverse the ISI penalty induced by pre-filtering in a non-coherent OOK system. The correlation induced by pre-filtering can be seen in the constellation diagram, as shown in Fig. 8(a), where a single point in the typical QPSK constellation is transformed or converted into nine points. These four groups of 3×3 or $4 \times (3 \times 3)$ constellations are caused by the correlation between a symbol and its two nearest neighbors in the QPSK signal [14]. Significant penalty is expected if a single-symbol detection algorithm is used. On the other hand, the MAP algorithm is able to take advantage of the pre-filtering-induced symbol correlation in a detection scheme based on multiple symbols. Joint detection reduces the penalty from over-filtering in cases where the crosstalk from neighboring channels is small. With the MAP detection algorithm, the ISI-heavy $4 \times (3 \times 3)$ constellation can be compensated back to the typical QPSK constellation, as shown in Fig. 8(b) [14].

Fig. 9 shows the back-to-back performance for a single channel (with bandwidth constraining) and WDM at 400% SE after MAP detection. With MAP detection, the filtering penalty was reduced to only 2.2 dB (at 10-dB OSNR) for single channel (with bandwidth constraining), and the performance reached $\sim$12.8 dB. For the WDM case (25-GHz channel spacing),

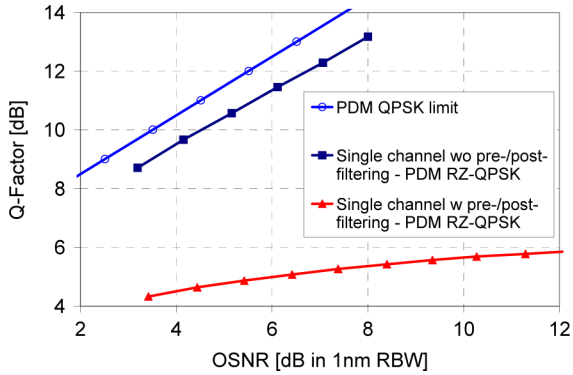

Fig. 7. Back-to-back performance comparison—with and without pre-/post-filtering for single channel.

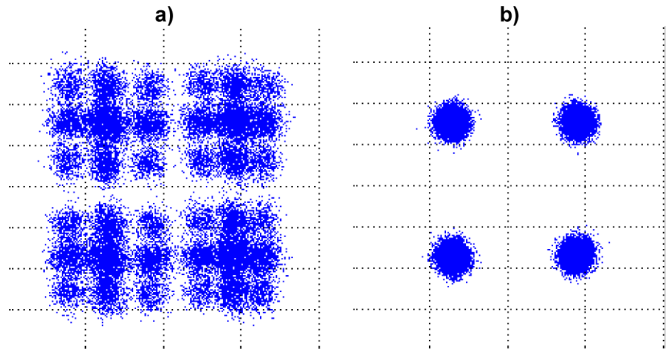

Fig. 8. (a) 25-GHz bandwidth-constrained 112-Gb/s PDM RZ-QPSK shows complex constellation [for 1 pol. with the corresponding optical spectrum shown in Fig. 6(d)]. (b) MAP detection algorithm recovers the constellation back to that of a typical QPSK signal.

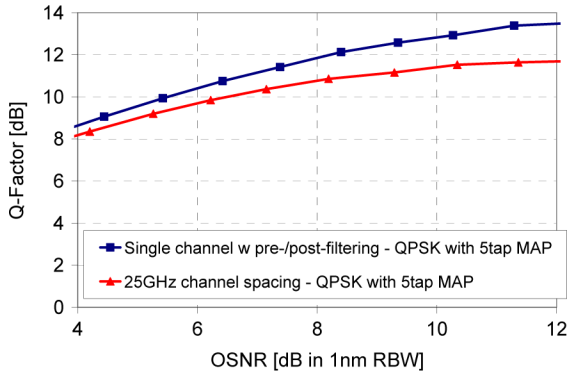

Fig. 9. Back-to-back performance comparison showing crosstalk penalty for 400% SE (with MAP detection).

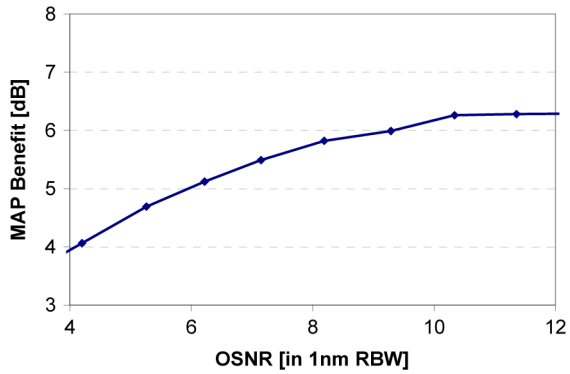

Fig. 10. MAP benefit for 25-GHz spaced 28-Gbaud PDM-RZ-QPSK.

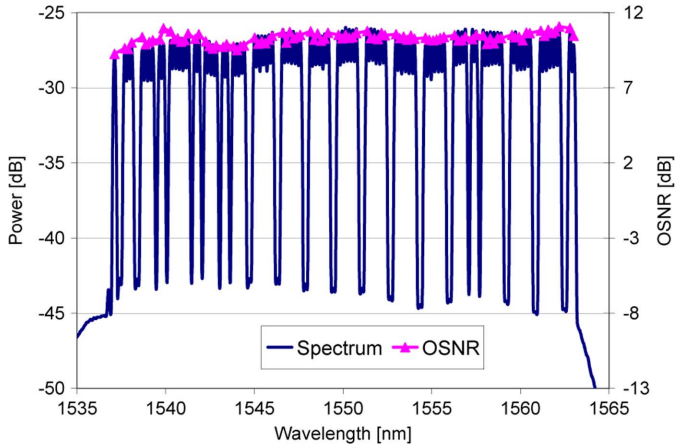

Fig. 11. Optical spectrum and OSNR (in 1 nm RBW) after 4370 km.

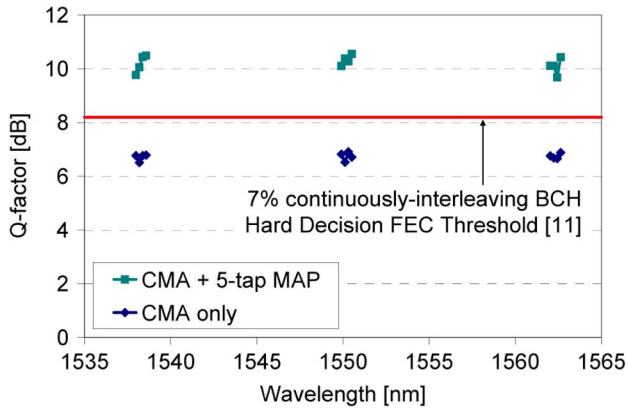

Fig. 12. Q-factor after 4370 km (400% SE) with different detection schemes.

the performance with MAP detection was ∼11.5 dB; a 6-dB MAP benefit compared with single-symbol QPSK detection, as shown in Fig. 10. Therefore, it is possible to achieve $>$ 400% SE with aggressive pre-filtering and MAP detection for the PDM-RZ-QPSK modulation format. In addition, Fig. 10 shows that MAP benefit is ONSR dependent. At lower OSNR, MAP benefits start to reduce, due to more and more noise-induced penalty.

VI. 100-GHz Transmission Over 4370 km With 400% SE Using Bandwidth-Constrained PDM RZ-QPSK

Fig. 11 shows the received optical spectrum and OSNR with flat launch after 4370-km transmission. The original 96 DFB lasers from the 300% SE experiment were rearranged in groups of 6 to create 25-GHz channel spacing covering the full bandwidth (with gaps). There were no more than two channels missing in a single loading gap. Similar to previous measurements, the eight ECLs were tuned to the measurement region and the corresponding DFBs were turned off during the performance measurement. We experimentally confirmed that a decorrelated four-rail transmitter setup performed very similar to the two-rail setup, as shown in Fig. 1 with 25-GHz channel spacing.

Fig. 12 shows the performance of select channels from three locations across the band with and without MAP detection after 4370 km transmission. The five-tap MAP detection algorithm provides $>$3-dB benefit over CMA alone for all channels. We also compared the performance when using a different number of taps for the MAP detection algorithm. Compared with the five-tap MAP detection scheme, 3-tap MAP resulted in ∼2-dB lower performance [14]. Seven-tap MAP on the other hand requires much longer decoding time. To balance performance and decoding time we therefore use five-tap MAP for the rest of the paper. Similar to the 300% SE experiment, more EDFA power would have improved performance.

We also compared the performance of PDM RZ-QPSK and PDM NRZ-QPSK with pre- and post-filtering. Bandwidth-constrained PDM RZ-QPSK outperformed bandwidth-constrained PDM NRZ-QPSK by ∼0.5 dB even with the aggressive pre-filtering, as shown in Fig. 13.

VII. Transmission Distance Limit

Fig. 14 shows the achievable transmission distance for a channel near 1550 nm with optimum transmitter pre-emphasis for both 300% SE and 400% SE. For 300% SE, we achieved ∼14 000 km with Q -factor $>$10 dB commensurate with ∼300 000 ps/nm of accumulated dispersion. For 400% SE, the transmission distance can still reach ∼5000 km with Q-factor $>$10 dB.

VIII. Discussion

The spectral efficiencies demonstrated in this paper are plotted in Fig. 15 for comparison with previous generations

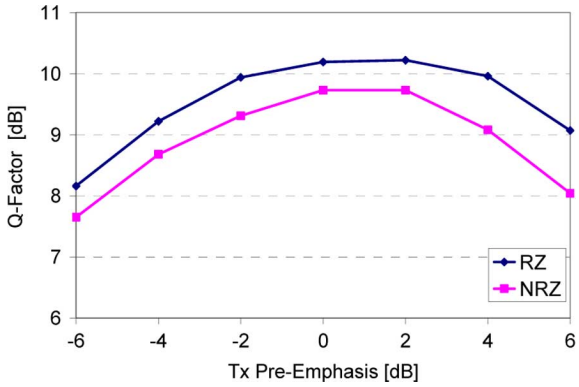

Fig. 13. Performance comparison of PDM RZ-QPSK and PDM NRZ-QPSK.

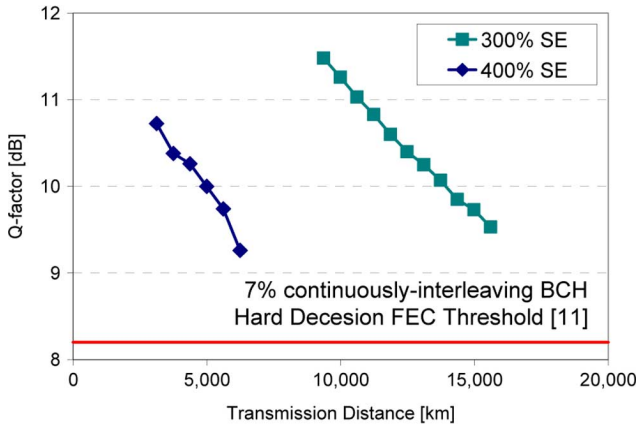

Fig. 14. Q-factor versus transmission distance for 300% and 400% SE near 1550 nm.

of terminal equipment for undersea cable systems and the SE limits for several memory-less modulation formats [10], [14]. For a fair comparison, the SE definition was modified to "Line Bit Rate/Channel Spacing/(1 + FEC overhead)" instead of "User Bit Rate/Channel Spacing" for this section only. With the modified definition, the 300% SE and 400% SE in our experiment would be 314% (112 Gb/s at 33-GHz channel spacing with 7% FEC overhead) and 419% (112 Gb/s at 25-GHz channel spacing with 7% FEC overhead), respectively.

At first glance one might conclude that this 419% result exceeds the 400% SE limit for the PDM-QPSK modulation format [15]; however, by reducing the signal bandwidth through prefiltering and maintaining the same information content as for QPSK through multi-symbol detection we were able to exceed the 400% SE limit of the **memory-less** PDM-QPSK modulation format [16]. However, the 419% SE (achieved with bandwidth-constrained PDM-QPSK and MAP detection) is still far from the Shannon limit as also shown in Fig. 15.

Furthermore, Fig. 15 shows that this new high SE result changes the trend of achieved SE versus required OSNR. In previous generations of terminal equipment for undersea communication systems, due to the more and more powerful FEC algorithms, the required OSNR decreased with increased SE as we transitioned from OOK to DBPSK modulation formats as shown by the red dashed line in Fig. 15. However, as we

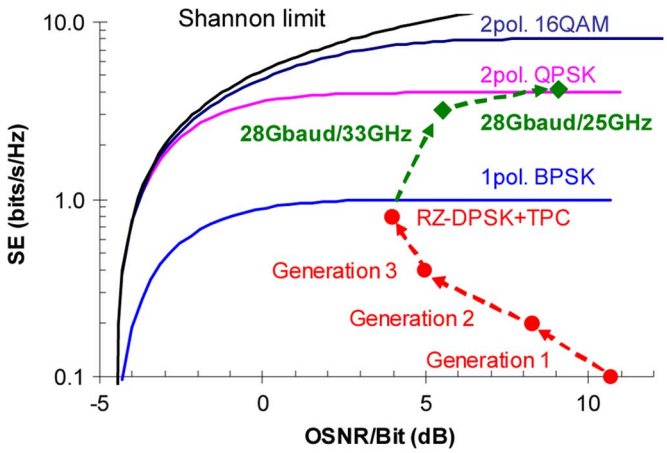

Fig. 15. SE versus required OSNR.

go to higher level modulation formats, the required OSNR increases with increasing SE as shown by the green dashed line. In our current experiments we used short spans (52 km) and larger effective area fibers (150 μm ^{2}) to enhance OSNR and minimize this trend.

We have demonstrated significant MAP detection benefits. In general, the MAP benefit depends on the operating OSNR, the channel spacing (i.e., ISI from the transmitter), linear crosstalk from neighboring channels, the number of taps, etc. The lower the received OSNR, the smaller the MAP benefit as noise induced penalty dominates the overall penalty, as shown in Fig. 10. The larger the ISI and the smaller the crosstalk from neighboring channels from the transmitter, the larger the MAP benefit. Moreover, the higher the number of taps in MAP, the more MAP benefit. However, the number of taps is limited by the physical implementation complexity and power consumption of the high-speed electronics.

IX. Conclusion

We demonstrated 96 × 112-Gb/s transmission with 300% SE over 10 610 km using a bandwidth-constrained PDM-RZ-QPSK modulation format in conjunction with a MAP detection algorithm. Aggressive filtering reduced crosstalk from neighboring channels and induced correlation between symbols. Our MAP detection algorithm can reduce the ISI-induced penalty by taking advantage of the symbol correlation. With >3-dB MAP detection benefit, we also demonstrated 400% SE for 112-Gb/s signals at 25-GHz channel spacing over 4370 km. Short amplifier spacing (52 km) and larger effective area fibers (150 μm ^{2}) were used to maintain a high received OSNR.

References

[1] G. Charlet, M. Salsi, P. Tran, M. Bertolini, H. Mardoyan, J. Renaudier, O. Bertran-Pardo, and S. Bigo, "72×100 Gb/s transmission over transoceanic distance, using large effective area fiber, hybrid Raman-erbium amplification and coherent detection," presented at the Optical Fiber Communication Conf. and Exposition and National Fiber Optic Engineers Conf 2009 , San Diego, CA, Paper PDPB6.

[2] M. Salsi, H. Mardoyan, P. Tran, C. Koebele, E. Dutisseuil, G. Charlet, and S. Bigo, "155 × 100 Gbit/s coherent PDM-QPSK transmission over 7 200 km," presented at the Eur. Conf. and Exhibition Optical Communication 2009 , Vienna, Austria, Paper PD2.5.

[3] H. Masuda, E. Yamazaki, A. Sano, T. Yoshimatsu, T. Kobayashi, E. Yoshida, Y. Miyamoto, S. Matsuoka, Y. Takatori, M. Mizoguchi, K. Okada, K. Hagimoto, T. Yamada, and S. Kamei, "13.5-Tb/s (135 × 111-Gb/s/ch) no-guard-interval coherent OFDM transmission over 6 248 km using SNR maximized second-order DRA in the extended L-band ," presented at the Optical Fiber Communication Conf. and Exposition (OFC) and the National Fiber Optic Engineers Conf. 2009, San Diego, CA, Paper PDPB5.

[4] S. Chandrasekhar, X. Liu, B. Zhu, and D. W. Peckham, "Transmission of a 1.2-Tb/s 24-carrier no-guard-interval coherent OFDM superchannel over 7200-km of ultra-large-area fiber," presented at the Eur. Conf. and Exhibition Optical Communication 2009 , Vienna, Austria, 2009, Paper PD2.6.

[5] J.-X. Cai, Y. Cai, C. R. Davidson, D. G. Foursa, A. Lucero, O. Sinkin, W. Patterson, A. Pilipetskii, G. Mohs, and N. Bergano, "Transmission of 96 × 100 G bandwidth-constrained PDM RZ QPSK channels with 300% spectral efficiency over 10 610 km and 400% spectral efficiency over 4 370 km," presented at the Optical Fiber Communication Conf. and Exposition and the National Fiber Optic Engineers Conf. 2010, San Diego, CA, Paper PDPB10.

[6] Q. Yu, L.-S. Yan, S. Lee, Y. Xie, and A. E. Willner, "Loop-synchronous polarization scrambling technique for simulating polarization effects using recirculating fiber loops," *J. Lightw. Technol.*, vol. 21, no. 7, pp. 1593 –1600, Jul. 2003.

[7] C. Laperle, B. Villeneuve, Z. Zhang, D. McGhan, H. Sun, and M. O'Sullivan, "WDM performance and PMD tolerance of a coherent 40-Gbit/s dual-polarization QPSK transceiver ," *J. Lightw. Technol.*, vol. 26, no. 1, pp. 168 –175, Jan. 2008.

[8] A. J. Viterbi and A. M. Viterbi, "Nonlinear estimation of PSK-modulated carrier phase with application to burst digital transmission ," *IEEE Trans. Inf. Theory*, vol. IT-29, no. 4, pp. 543–551, Jul. 1983.

[9] Y. Cai, D. G. Foursa, C. R. Davidson, J.-X. Cai, O. Sinkin, M. Nissov, and A. Pilipetskii, "Experimental demonstration of coherent MAP detection for nonlinearity mitigation in long-haul transmissions," presented at the Optical Fiber Communication Conf. and Exposition and National Fiber Optic Engineers Conf. 2010, San Diego, CA, Paper OTuE1 .

[10] Y. Cai, "Coherent detection in long-haul transmission systems," presented at the Optical Fiber Communication Con. and Exposition and the National Fiber Optic Engineers Conf. 2008, San Diego , CA, 2008, Paper OTuM1.

[11] F. Chang, K. Onohara, and T. Mizuochi, "Forward error correction for 100 G transport networks," *IEEE Commun. Mag.*, vol. 48, no. 3, pp. 48 –55, Mar. 2010.

[12] S. Zhang, X. Li, P. Kam, C. Yu, and J. Chen, "Pilot-assisted decision-aided maximum-likelihood phase estimation in coherent optical phase-modulated systems with nonlinear phase noise," *IEEE Photon. Technol. Lett.*, vol. 22, no. 6, pp. 380–382, Mar. 2010.

[13] N. Alic, M. Karlsson, M. Skold, O. Milenkovic, P. Andrekson, and S. Radic, "Joint statistics and MLSD in filtered incoherent high-speed fiber-optic communications ," *J. Lightw. Technol.*, vol. 28, no. 10, p. 168 , May 2010.

[14] Y. Cai, J.-X. Cai, C. R. Davidson, D. Foursa, A. Lucero, O. Sinkin, A. Pilipetskii, G. Mohs, and N. S. Bergano, "High spectral efficiency long-haul transmission with pre filtering and maximum *a posteriori* probability detection," presented at the Eur. Conf. and Exhibition on Optical Communication 2010 , Torino, Italy, Paper We.7.C.4..

[15] R.-J. Essiambre, G. Kramer, P. J. Winzer, G. J. Foschini, and B. Goebel, "Capacity limits of optical fiber networks," *J. Lightw. Technol.*, vol. 28, no. 4, pp. 662 –701, Feb. 2010.

[16] Y. Cai, J.-X. Cai, A. Pilipetskii, G. Mohs, and N. S. Bergano, "Spectral efficiency limits of pre-filtered modulation formats," *Opt. Exp.*, vol. 18, no. 19, pp. 20273–20281 , 2010.

Jin-Xing Cai (S'97–M'00–SM'05–F'11) received the B.S. and M.S. degrees in electronic engineering from Tsinghua University, Beijing, China, in 1988 and 1994, respectively, and the Ph.D. degree in electrical engineering from the University of Southern California, Los Angeles, CA in 1999.

In 1999, he joined Tyco Submarine Systems Ltd. (now Tyco Electronics Subsea Communications LLC), Eatontown, NJ. His current research interests include ultra long-haul transmission of high-speed DWDM channels with massive system aggregate capacity.

Yi Cai (S'98–M'01) received the B.S. degree in optical engineering from Beijing Institute of Technology, Beijing, China, in 1992, the M.S. degree in electrical engineering from Shanghai Institute of Technical Physics, Chinese Academy of Sciences, Shanghai, China, in 1998, and the Ph.D. degree in electrical engineering from the University of Maryland Baltimore County, Baltimore, in 2001.

In 2001, he joined Tyco Electronics Subsea Communications, Eatontown, NJ. His current research interests include coherent detection, forward error correction, and advanced modulation formats in optical fiber communications.

Carl R. Davidson, biography not available at the time of publication.

Dmitri G. Foursa (SM'10) was born in Moscow, Russia, in 1960. He received the Diploma degree in physics and Ph.D. degree from Moscow Physical and Technical Institute, Moscow, Russia, in 1983 and 1992, respectively.

He was a Research Fellow with the General Physics Institute, Moscow, Russia. During 1990–1991, he was an Academic Visitor with Imperial College, London, U.K., concentrating on erbium-doped fiber lasers and high-repetition-rate trains of solitons. During 1994–1995, he held a Postdoctoral fellowship from SSTC at Université Libre de Bruxelles (ULB), Belgium, where, from 1995 to 1999, he was a Senior Research Scientist investigating experimentally and numerically dark and gray solitons and their Raman amplification in optical fibers, erbium-fiber lasers, and high-bit-rate pulse shaping techniques. In 1999, he joined Tyco Electronics Subsea Communications, where, as a Distinguished Member of Technical Staff, his current research concerns advanced optical amplifiers and transmission issues in submarine telecommunications.

Dr. Foursa is a Senior Member of the Photonics Society.

Alan J. Lucero was born on December 18, 1949. He received the M.S. and Ph.D. degrees in physics from the University of Connecticut, Storrs, in 1989 and 1993, respectively.

In 1995, he completed a two-year postdoctoral fellowship at Bell Laboratories, Crawford Hill, NJ, and subsequently accepted a Member of Technical Staff position at AT&T Advanced Technologies Systems, Whippany, NJ, where he was engaged in research on the development of low power consumption erbium-doped fiber lasers and system design. In 1997 he left to assist in the establishment of the Photonics Research and Test Center for Corning, Inc., in Somerset, NJ. In 2000, he joined Tyco Electronics Subsea Communications, Eatontown, NJ, where he is engaged in research on linear and nonlinear properties of 10- and 40-Gb/s transport over novel dispersion maps.

Dr. Lucero is a Member of Phi Beta Kappa.

Oleg V. Sinkin (M'01) was born in Protvino, Russia, in 1976. He received the M.S. degree (*cum laude*) in applied physics and mathematics from Moscow Institute of Physics and Technology, Moscow, Russia, in 1999, and the Ph.D. degree in electrical engineering from the University of Maryland Baltimore County in 2006.

During 1996–1999, he was a Research Engineer at IRE-POLUS, Moscow (IPG Photonics), where he was involved in designing fiber lasers and amplifiers. During his Ph.D. studies, he was engaged in research on developing analytical and numerical techniques to model optical fiber communications, studying nonlinear propagation effects in optical fibers and modeling experiments. He is currently a Senior Member of the System Modeling and Signal Processing Research, Tyco Electronics Subsea Communications, Eatontown, NJ.

Dr. Sinkin has been a member of the Photonics Society since 2001.

William W. Patterson was born in Maryville, TN. He received the Bachelor of Science degree in electrical engineering from the University of Tennessee, Knoxville, in 1980, and the Master of Science Degree in computer science from the University of Illinois, Urbana, in 1988.

In 1980, he joined Western Electric, where he was involved in designing computer-automated test equipment, and then SLC Digital Loop Carrier circuit packs. In 1988, he transferred to the Submarine Systems division of AT&T Bell Laboratories, which was purchased by Tyco Electronics Subsea Communications, Eatontown, NJ in 1997, where he has since been involved in the testing of undersea systems, and in the design of equipment used to test undersea systems.

Mr. Patterson is a member of Tau Beta Pi.

Alexei N. Pilipetskii received the M.S. degree in physics from Moscow State University, Moscow, Russia, in 1985, and the Ph.D. degree from the General Physics Institute Academy of Sciences, Moscow, Russia, in 1990 for the research in the nonlinear fiber optics.

From 1985 to 1994, he was with the General Physics Institute, Russia. From 1994 to 1997, he was with the UMBC, where his interest shifted to the fiber optic data transmission. Since 1997, he has been with Tyco Electronics Subsea Communications, Eatontown, NJ, where he has been engaged on a number of research and development projects. He is currently the Director of a research group with the focus on the next-generation technologies for the undersea transmission systems.

Georg Mohs (M'05–SM'05) received his Diploma degree in physics from the University of Dortmund, Germany, in 1993, and the M.S. and Ph.D. degrees in optical sciences from the University of Arizona, Tucson, in 1995 and 1996, respectively.

He was a Research Associate at the University of Tokyo, Japan, where he was engaged in research on semiconductor optics and ultrafast carrier dynamics in semiconductors. In 1998, he joined the Optical Networks Research and Development Group of Siemens in Munich, Germany, where was engaged in research on terrestrial optical communication systems. In 2001, he joined Tyco Telecommunications (now Tyco Electronics Subsea Communications, LLC) Laboratories, Eatontown, NJ, as a Distinguished Member of the Technical Staff. He is now the Director of the Transmission Research group, leading the forward looking experimental work in high-capacity undersea optical communication systems.

Neal S. Bergano (S'80–M'88–SM'90–F'99) received the B.S. degree in electrical engineering from the Polytechnic Institute of New York, New York, in 1981, and the M.S. degree in electrical engineering and computer science from the Massachusetts Institute of Technology, Cambridge, in 1983.

In 1981, he joined the technical staff of Bell Labs' undersea systems division. In 1992, he was named a Distinguished Member of the Technical Staff of AT&T Bell Labs. In 1996 he was promoted to AT&T Technology Consultant. In 1997, he was promoted to AT&T Technology Leader. He is currently a Managing Director of the System Research and Network Development at Tyco Electronics Subsea Communications ("TE SubCom") LLC, Eatontown, NJ. He holds 31 U.S. patents in the area of optical fiber transmission systems. His main career has been devoted to the understanding of how to improve the performance and transmission capacity of long-haul optical fiber systems, including the use of wavelength division multiplexing in optical amplifier based systems.

Mr. Bergano is a Fellow of the Optical Society of America (OSA), AT&T, and Tyco Electronics. He is on the Board of Directors for the OSA, and has served on the Board of Governors for the IEEE Lasers and Electro-Optics Society from 1999 to 2001. He is a long-time volunteer and supporter of the Optical Fiber Communication Conference and Exposition and the National Fiber Optic Engineers Conference (OFC/NFOEC) meeting, which includes general chair and technical chair in 1999 and 1997, Chair of the steering committee from 2000 to 2002, and is currently the Chair of OFC/NFOEC's long-range planning committee. He is the recipient of the 2002 John Tyndall Award, for outstanding technical contributions to and technical leadership in the advancement of global undersea fiber-optic communication systems.